1521-0111/101/5/309–321$35.00
MOLECULAR PHARMACOLOGY

dx.doi.org/10.1124/molpharm.121.000419
Mol Pharmacol 101:309–321, May 2022

Serotonin-Mediated Activation of Serotonin Receptor Type 1 Oppositely Modulates Voltage-Gated Calcium Channel Currents in Rat Sensory Neurons Innervating Hindlimb Muscle

Laura Anselmi, Joyce S. Kim, Marc P. Kaufman, Shouhao Zhou, and Victor Ruiz-Velasco

Department of Anesthesiology and Perioperative Medicine (L.A., V.R.-V.) and Heart and Vascular Institute (J.S.K., M.P.K.), Penn State College of Medicine, Hershey, Pennsylvania; and Department of Public Health Sciences Division of Biostatistics and Bioinformatics, Penn State Cancer Institute, Next-Generation Therapies, Hershey, Pennsylvania (S.Z.)

Received September 27, 2021; accepted February 5, 2022

ABSTRACT

Serotonin (5-HT) is a multifaceted neurotransmitter that has been described to play a role as a peripheral inflammatory mediator when released in ischemic or injured muscle. Dorsal root ganglia (DRG) neurons are key sensors of noxious stimuli that are released under inflammatory conditions or mechanical stress. Little information is available on the specific 5-HT receptor subtypes expressed in primary afferents that help regulate reflex pressor responses. In the present study, the whole-cell patch-clamp technique was employed to examine the modulation of voltage-gated calcium channel (Ca_V) 2.2 currents by 5-HT and to identify the 5-HT receptor subtype(s) mediating this response in acutely dissociated rat DRG neurons innervating triceps surae muscle. Our results indicate that exposure of 1,1'-dioctadecyl-3,3,3′,3′-tetramethylindocarbocyanine perchlorate (DiI)-labeled DRG neurons to 5-HT can exert three modulatory effects on Ca_V currents: high inhibition, low inhibition, and enhancement. Both 5-HT-mediated inhibition responses were blocked after pretreatment with pertussis toxin (PTX), indicating that 5-HT receptors are coupled to $Ca_V2.2$ via $G\alpha_{i/o}$ protein subunits. Application of selective serotonin receptor type 1 (5-HT1) agonists revealed that modulation of $Ca_V2.2$ currents occurs primarily after 5-HT1A receptor subtype stimulation and minimally from 5-HT1D activation. Finally, the intrathecal administration of the selective 5-HT1A receptor agonist, 8-hydroxy-2-(di-n-propylamino)tetralin (8-OH-DPAT), significantly ($P < 0.05$) decreased the pressor response induced by intra-arterial administration of lactic acid. This suggests that 5-HT1A receptors are expressed presynaptically on primary afferent neurons innervating triceps surae muscle. Our findings indicate that preferential stimulation of 5-HT1 receptors, expressed on thin fiber muscle afferents, serves to regulate the reflex pressor response to metabolic stimuli.

SIGNIFICANCE STATEMENT

The monoamine serotonin (5-HT), released under ischemic conditions, can contribute to the development of inflammation that negatively affects the exercise pressor reflex. The 5-HT receptor subtype and signaling pathway that underlies calcium channel modulation in dorsal root ganglia afferents, innervating hindlimb muscles, are unknown. We show that 5-HT can either block (primarily via serotonin receptor type 1 (5-HT1)A subtypes) or enhance voltage-gated calcium channel ($Ca_V2.2$) currents. Our findings suggest 5-HT exhibits receptor subtype selectivity, providing a complexity of cellular responses.

Introduction

The monoamine neurotransmitter serotonin (5-HT) regulates a number of physiologic and pathophysiological processes (Hornung, 2003; De Ponti, 2004; Watts et al., 2012; Švob Štrac et al., 2016) and is known to play an important role in the development and progression of peripheral artery disease (PAD) (Stojanović et al., 2017). In fact, a recent study found that 5-HT serum levels were markedly elevated in patients with PAD (Senol and Es, 2015), implying it may play a role in the development and/or progression of this disease. It has also been suggested that 5-HT released onto inflamed or injured muscle contributes to hyperalgesia via sensitization of thin fiber muscle afferents (Sommer, 2004; Shajib and Khan, 2015). In addition, several studies have shown that 5-HT receptors are expressed in central, autonomic, and sensory neurons along pain pathways (Bardin, 2011; Cortes-Altamirano et al., 2018).

The actions exerted by 5-HT occur through stimulation of a number of 5-HT receptors. The 5-HT receptor family is made up of seven families or subtypes, serotonin receptor type 1–7

This article was supported by National Institutes of Health National Heart, Lung, and Blood Institute [Grant P01-HL134609].
No author has an actual or perceived conflict of interest with the contents of this article.
dx.doi.org/10.1124/molpharm.121.000419.

ABBREVIATIONS: Ca_V, voltage-gated calcium channel; CDK5, cyclin-dependent kinase 5; CH_3SO_3H, methanesulphonic acid; CTX, cholera toxin; DiI, 1,1'-dioctadecyl-3,3,3′,3′-tetramethylindocarbocyanine perchlorate; DRG, dorsal root ganglia; 5-HT, serotonin; 5-HT1–7, serotonin receptor type 1–7; I-V, current-voltage; MAP, mean arterial pressure; NAS-181, (2R)-2-[[[3-(4-Morpholinylmethyl)-2H-1-benzopyran-8-yl]oxy]-methyl]morpholine dimethanesulfonate; 8OH-DPAT, 8-hydroxy-2-(di-n-propylamino)tetralin; PAD, peripheral artery disease; PTX, pertussis toxin.

(5-HT1–7). With the exception of the ligand-gated ion channel, 5-HT3, all 5-HT receptors are members of the G-protein coupled receptor superfamily (Derkach et al., 1989; Hoyer et al., 2002; Cortes-Altamirano et al., 2018). 5-HT mediates its effects by coupling 5-HT receptors to members of PTX-sensitive $G\alpha_{i/o}$ subunits or cholera-toxin (CTX)-sensitive $G\alpha_s$ subunits and/or $G\alpha_{q/11}$ family of heterotrimeric G proteins (Raymond et al., 2001; Millan et al., 2008). The $G\alpha_{i/o}$-coupled 5-HT-mediated activation of 5-HT receptors results in inhibition of voltage-gated Ca^{2+} (Ca_V) channels, activation of G protein inwardly rectifying K^+ channels and negative coupling to adenylyl cyclase (Raymond et al., 2001; Millan et al., 2008).

The purpose of the present study was to first determine the modulation of $Ca_V2.2$ currents by 5-HT and the receptor subtypes expressed in dorsal root ganglion (DRG, L_4-L_5) neurons that innervate rat hindlimb triceps surae muscle. Second, the identification of the signaling elements that couple to $Ca_V2.2$ (N-type) channels was performed. Previously, we reported that $Ca_V2.2$ channels are the predominant Ca^{2+} channel subtype in DRG neurons that innervate the triceps surae muscle (Ramachandra et al., 2013). Furthermore, $Ca_V2.2$ channels regulate transmitter release of peripheral sensory neurons involved in pain transmission (Westenbroek et al., 1998). Previous studies have reported that sensory neurons express five 5-HT receptor subtypes (Daval et al., 1987; Cardenas et al., 1997a; Cardenas et al., 1997b; Chen et al., 1998; Classey et al., 2010). However, the specific 5-HT receptor subtype and signaling pathway that underlies Ca^{2+} channel modulation in DRG afferents, which regulate the exercise pressor reflex, have not been previously characterized.

Materials and Methods

Animals. All procedures were conducted in accordance with National Institutes for Health guidelines with the approval of the Penn State University College of Medicine Institutional Animal Care and Use Committee and according to journal policies and regulations on animal experimentation. Adult male Sprague-Dawley rats (Charles River Laboratories, Wilmington, MA) were used after being acclimated for at least seven days in a light controlled-room (12-hour light/12-hour dark cycle) with ad libitum access to standard rat chow and water.

DRG Neuron Labeling and Isolation. DRG neurons were isolated as described previously (Farrag et al., 2017). Briefly, the neurons innervating the triceps surae muscles were identified using the retrograde fluorescent neuronal tracer DiI (1,1'-dioctadecyl-3,3,3′,3′-tetramethylindocarbocyanine perchlorate; Thermo-Fisher Scientific, Carlsbad, CA). Three days prior to DRG neuron isolation, 100 μl of DiI (3% in DMSO) were injected into the triceps surae muscles. On the day the neurons were isolated, the rats were anesthetized with carbon dioxide and euthanized by decapitation. The lumbar DRG (L_4–L_5) were dissected, and the connective tissue was then cleared in ice-cold Hanks' balanced salt solution (Sigma-Aldrich, St. Louis, MO). The ganglia were then enzymatically dissociated in Earle's balanced salt solution (Sigma-Aldrich) containing collagenase Type D (0.6 mg/ml; Roche Diagnostics Corp. Indianapolis, IN), trypsin (0.4 mg/ml, Worthington, Lakewood, NJ), and DNase (0.1 mg/ml; Alfa Aesar, Ward Hill, MA) in a water bath for 45 minutes at 35°C. Afterward, the neurons were vigorously shaken and centrifuged twice for 6 minutes at 50 × g and then placed in minimum essential medium (Thermo-Fisher Scientific) supplemented with 10% FBS (VWR, Radnor, PA), 1% glutamine, and 1% penicillin-streptomycin (both from Thermo-Fisher). Finally, the neurons were plated onto 35 mm poly-L-lysine coated dishes and placed overnight in a humidified incubator (5% carbon dioxide/95% air) at 37°C. In some experiments, DRG neurons were pretreated overnight with 500 ng/ml PTX or 500 ng/ml CTX, both from List Biologic Laboratories., Campbell, CA.

Whole-Cell Patch-Clamp. Ca^{2+} currents of DiI-labeled DRG neurons were recorded employing the whole-cell variant of the patch-clamp technique. The recording pipettes, made of borosilicate glass (King Precision Glass, Claremont, CA), were pulled with a P-97 micropipette puller (Sutter Instrument Co., Novato, CA). The Ca^{2+} current recordings were acquired with an Axopatch 200B amplifier (Molecular Devices, Sunnyvale, CA), analog filtered at frequency 2 kHz (−3dB, 4-pole low-pass Bessel filter), and digitized (2–5 kHz) with custom-designed F6 software (developed by Stephen R. Ikeda, National Institutes of Health/National Institute on Alcohol Abuse and Alcoholism) equipped with an 18-bit analog-to-digital converter board (ITC-18, HEKA Instruments, Inc., Bellmore, NY). Both cell membrane capacitance and pipette series resistance were electronically compensated (80%–85%).

The Ca^{2+} currents were evoked with either a single- or the triple-pulse voltage protocol (Ikeda, 1991; Lu and Ikeda, 2016). The single-pulse voltage protocol consisted of a 70-millisecond test pulse to +10 mV from a holding potential of −80 mV applied every 10 seconds. The triple-pulse voltage protocol consists of a 25-millisecond test pulse to +10 mV (prepulse) followed by a 50-millisecond depolarizing conditioning test pulse to +80 mV, a brief return to −80 mV and followed by a 25-millisecond test pulse to +10 mV (postpulse). The current-voltage (I-V) relationships were obtained with a series of 70-millisecond depolarizing steps to various test pulse potentials from a holding potential of −80 mV (from −60 to +60 mV, 5 mV steps). Ca^{2+} current amplitude was measured isochronally 3–5 milliseconds after the initiation of each pulse.

Recording Solutions and Agents. The Ca^{2+} current bath recording solution (external) contained (in mM): TEA-hydroxide (OH) 145, methanesulphonic acid (CH_3SO_3H) 140, HEPES 10, glucose 15, calcium chloride ($CaCl_2$) 10 and tetrodotoxin 0.0003, to pH 7.4 with TEA-OH. Two different pipette (internal) solutions were employed, and there were no overt differences between the Ca^{2+} current recordings obtained. The first contained (in mM): N-methyl-D-glucamine 80, TEA-OH 20, EGTA 11, HEPES 10, $CaCl_2$ 1, cesium chloride 20, cesium hydroxide 40, adenosine 5'-triphosphate magnesium 4, guanosine 5'-triphosphate disodium salt 0.3 and creatine phosphate 14, to pH 7.2 with CH_3SO_3H. The second contained (in mM): N-methyl-D-glucamine 120, TEA-OH 20, EGTA 11, HEPES 10, $CaCl_2$ 1, adenosine 5'-triphosphate magnesium 4, guanosine 5'-triphosphate disodium salt 0.3 and creatine phosphate 14, to pH 7.2 with CH_3SO_3H. Stock solutions of 5-HT (Sigma-Aldrich), (3R)-3-(Dicyclobutylamino)-8-fluoro-3,4-dihydro-2H-1-benzopyran-5-carboxamide hydrochloride (NAD 299 hydrochloride; serotonin receptor type 1 [5-HT1A] antagonist) and 1-[2-[4-(4-Fluorobenzoyl)-1-piperidinyl]ethyl]-1,3-dihydro-3,3-dimethyl-2H-indol-2-one hydrochloride (LY 310762 hydrochloride; 5-HT1D antagonist) (Tocris Cookson-Biotechne, Minneapolis, MN) were prepared in water; (2R)-2-[[[3-(4-Morpholinylmethyl)-2H-1-benzopyran-8-yl]oxy]methyl]morpholine dimethanesulfonate (NAS-181; 5-HT1B antagonist) (Tocris Cookson-Biotechne) was prepared in DMSO. All stock solutions were then diluted in the external solution to their final concentration prior to use. In experiments where neurons were treated with NAS-181, the control external solution contained DMSO (0.03%). Agonists and antagonists were applied to the neuron under study with a custom-designed gravity-fed perfusion system that was positioned approximately 100 μm from the cell.

In Vivo Pressor Response Measurement. One set of Sprague-Dawley rats was used for in vivo experiments designed to determine the effect of intrathecal injection of 5-HT receptor stimulation on the lactic acid-mediated increase in blood pressure (Kim and Kaufman, 2019). On the day of the experiment, the rats were anesthetized with a mixture of 2%–3% isoflurane and 100% oxygen. The trachea, both carotid arteries, jugular vein, and superficial epigastric artery were cannulated. Arterial blood

pressure was measured through the catheter placed in one carotid artery, and fluids and drugs were administered respectively through the catheters in the jugular vein and superficial epigastric artery. All intra-arterial injections of lactic acid were made in the catheter (PE-8) placed in the superficial epigastric artery. A snare was placed around the femoral artery and vein and was tightened before every intra-arterial injection. Laminectomy was performed to expose the L_4–L_6 spinal segments followed by an incision of the dura at the L_6. A saline-filled PE-8 catheter was inserted with its tip pointed toward the femoral artery. The rats were then placed in a Kopf customized spinal frame and stereotaxic instrument and were tilted nose up 25–30 degrees to minimize the spread of intrathecal-injected drug to the medulla. A rostral lumbar vertebra and the pelvis were clamped to hold the rat securely in place. A precollicular decerebration was then performed, the isoflurane anesthesia was terminated, and the lungs were subsequently ventilated with room air. The experimental protocol was initiated after the lungs were ventilated with room air for 60 minutea.

We examined the effect of intrathecal injection of 5-HT (25 μg) and also of a selective 5-HT1A receptor agonist, 8-hydroxy-2-(di-n-propylamino)tetralin (8OH-DPAT, 50 μg in 10 μl, Sigma-Aldrich), on the pressor response to lactic acid injection (12 mM in a 200 μl volume) into the superficial epigastric artery. The interval between intrathecal injection and arterial administration of lactic acid was 40 minutes. Stock solutions were prepared in saline for lactic acid and 5-HT; 6% DMSO was used to prepare 8OH-DPAT stock solution. Controls were implemented by testing the pressor response to lactic acid before and after intrathecal injection of either saline or 6% DMSO solution. In both cases, the pressor responses were not overtly affected (see *Results*). At the end of each experiment, Evans blue dye was injected in the intrathecal catheter and intra-arterially to look for evidence of spread of the dye to the medulla and to determine that lactic acid was delivered to the triceps surae muscle. In all experiments, arterial blood pressure (mmHg) and heart rate (beats/min) were displayed continuously in real-time with a Spike2 data acquisition system (Cambridge Electronic design).

Data Analysis. For data and statistical analysis, Igor Pro 6.0 (WaveMetrics, Lake Oswego, OR) and Prism 6.0 (GraphPad Software, San Diego, CA) were used, respectively. The data are expressed as mean ±S.E. or mean ±S.D. and evaluated using paired or unpaired two-tailed t tests. Graphs and current traces were generated with Igor Pro 6.0 and iDraw (Indeeo, Palo Alto, CA) software.

The concentration-response relationships were determined by the sequential application of the receptor agonist, 5-HT, in increasing concentrations. Two different concentrations were employed for each labeled neuron tested. The results were then pooled and the concentration-response curve for the high responder neurons was obtained with the Hill equation: $I = I_{max}/\{1 + (IC_{50}/[ligand])^{nH}\}$, where I is the Ca_V inhibition (%), I_{max} is the maximum Ca_V inhibition (%), IC_{50} is the half-inhibition concentration, [ligand] is the agonist concentration, and nH is the Hill coefficient.

As mentioned above, exposure of the DRG neurons to 5-HT (10 μM) led to four outcomes, two of which either exhibited high or low Ca^{2+} current inhibition (Fig. 1). Thus, to determine whether both of these responses represented a single or double cluster, we employed a random effects finite mixture regression model with Gaussian distributions (McLachlan and Peel, 2000). The bimodal response was transformed using a logit transformation and the dose-response curve was estimated for the cluster containing high responder neurons. This classification was binary (i.e., probabilities were not determined) so that there were no borderline cases or data dredging and, thus, maintaining an objective approach. Statistical Software *R* version 3.5.2 with package Mixtools version 1.2.0 was used for computation, and $P < 0.05$ was considered statistically significant. Nonresponder neurons were those in which 5-HT exposure produced no discernible effect on Ca^{2+} currents, whereas the neurons referred to as enhancers exhibited a minimum of 15% increase in Ca^{2+} currents.

Results

Differential Modulation of $Ca_V2.2$ Currents by 5-HT. In the first set of experiments, we examined the effect of 5-HT on $Ca_V2.2$ currents in rat DRG neurons that innervate triceps surae muscle. We reported previously that this Ca^{2+} channel subtype is the major Ca^{2+} ion carrier in this specific neuron subpopulation (Ramachandra et al., 2013; Hassan et al., 2014). Figure 1, Ai–Aiii illustrates examples of the three outcomes observed after the exposure of DiI-labeled DRG neurons to 5-HT (10 μM). Figure 1Ai is a time course of Ca^{2+} currents evoked every 10 seconds with a 70-millisecond test pulse to +10 mV from a holding potential of −80 mV. The numbered Ca^{2+} current traces (right) evoked with this paradigm correspond to those plotted (left). Prior to 5-HT application, the peak Ca^{2+} current amplitude was approximately 3.2 nanoamperes (black trace). Exposure to 5-HT led to a block of approximately 20% (red trace). The time course shown in Fig. 1Aii depicts the second outcome obtained from the exposure of 5-HT on $Ca_V2.2$ currents. It can be observed that application of 5-HT (green trace) led to an approximately 64% block of the peak current. Finally, the time course in Fig. 1Aiii shows that application of 5-HT led to an increase (blue trace) of $Ca_V2.2$ currents of approximately 15%. The pie graph in Fig. 1B summarizes the frequency of the four types of responses observed. Half of all neurons tested did not express 5-HT receptors, referred to as nonresponders. Additionally, 5-HT appeared to block the currents in two manners. The first, referred to as low responders, was observed in ~23% of DRG neurons tested. On the other hand, those with a higher $Ca_V2.2$ block, referred to as high responders, were observed in 13% of neurons tested (Fig. 1B). Both of these responses represented two separate clusters rather than variable responses of a single cluster (see *Methods*). Finally, in 14% of DRG neurons tested, 5-HT exposure caused an enhancement of $Ca_V2.2$ currents. This group of neurons was classified as enhancers.

Figure 2 depicts the I-V relationships for low responders (A) and high responders (B) before and during 5-HT (10 μM) exposure. The Ca^{2+} currents were evoked to various depolarizing steps every 5 seconds from a holding potential of −80 mV. The superimposed current traces, shown to the left, were elicited with test potentials from −40 to +5 mV. In both groups of neurons, the Ca^{2+} currents began to activate at approximately −35 mV and reached a peak at approximately +5 mV. Application of 5-HT led to $Ca_V2.2$ current inhibition of 15% (Fig. 2A) and 47% (Fig. 2B) for the low responder and high responder, respectively, at the peak current. Further, it can be observed that the relationship between $Ca_V2.2$ current inhibition (A,B) and test potentials depicts a bell-shaped profile during 5-HT application, suggesting that the modulation is voltage-dependent.

5-HT Concentration-Response Relationships. In the next set of experiments, the 5-HT concentration-response relationship for high responders' DRG neurons was determined. Figure 3A shows the time course of peak $Ca_V2.2$ current of a DiI-labeled, "high responder" DRG neuron before (traces 1 and 3) and during exposure to 0.01 μM (trace 2) and 10 μM (trace 4) 5-HT. Currents were evoked as described in

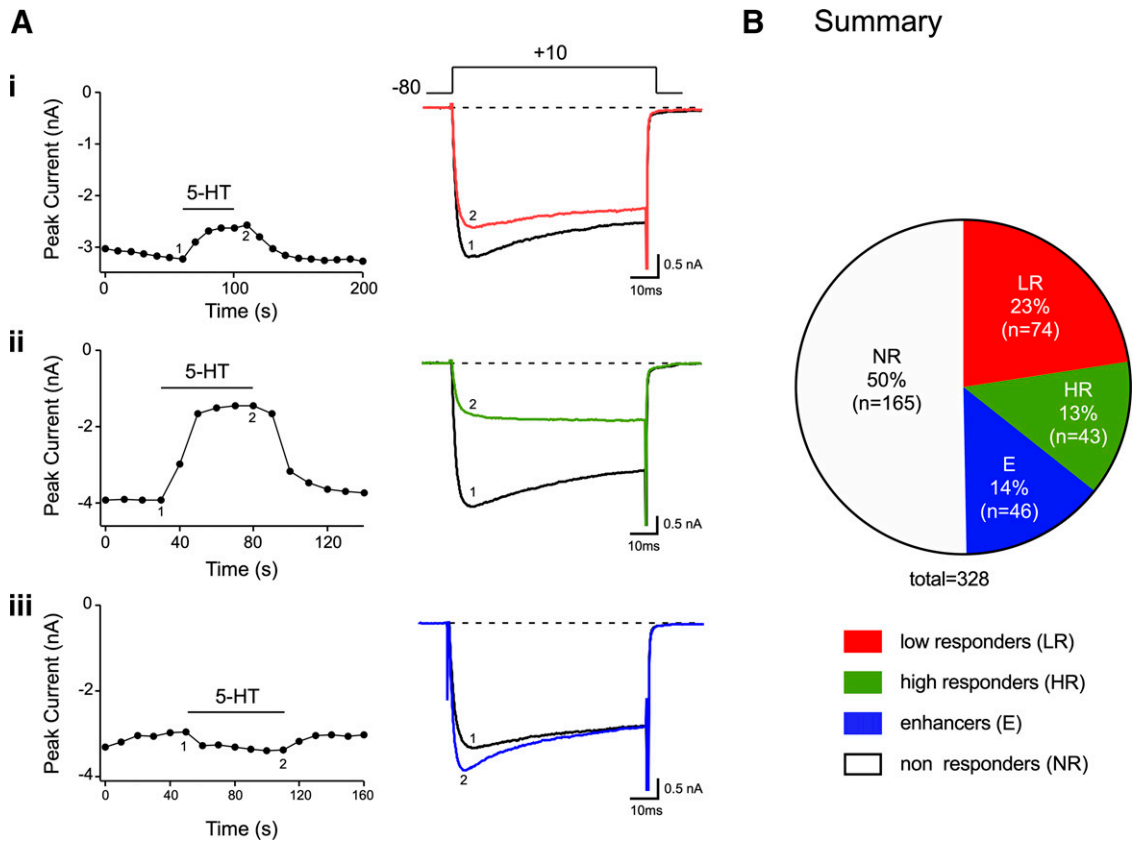

Fig. 1. 5-HT-mediated modulation of $Ca_V2.2$ currents of acutely isolated DiI-labeled DRG neurons. Time courses of peak $Ca_V2.2$ current amplitude after 5-HT (10 μM) exposure in DRG neurons with responses designated as low responders for low current inhibition (Ai), robust current inhibition, high responders (Aii), and current increase enhancers (Aiii). To the right are the superimposed current traces in the absence (1) or presence (2) of 5-HT. The currents were evoked every 10 seconds with the voltage protocol shown (A, top). (B) Summary pie chart showing the fractional representation of the effects mediated by 5-HT on $Ca_V2.2$ currents. The numbers in parentheses indicate the number of neurons tested.

Fig. 1. It can be observed that application of 0.01 μM 5-HT resulted in approximately a 2% block of the current. After a recovery period, exposure to 10 μM 5-HT caused an inhibition of the Ca^{2+} current by 64%. The 5-HT concentration-response relationship is shown in Fig. 3B. The data points were fit to the Hill equation, and the IC_{50} and Hill coefficient obtained were 0.25 μM and 1.3, respectively. We attempted to determine the concentration-response relationship for low responders, but the responses to 5-HT did not produce a discernible curve, and the nonlinear regression fit yielded incomplete confidence intervals. It should be noted that the maximal 5-HT-induced Ca^{2+} current block in low responders was observed with a concentration of 10 μM. Therefore, in the following experiments, this agonist concentration was employed.

G Protein Subunit Coupling of 5-HT Receptors to $Ca_V2.2$ Channels. In this set of experiments, we employed ADP-ribosylating bacterial exotoxins to determine the Gα protein subfamily involved in the signaling pathway of the 5-HT-mediated $Ca_V2.2$ current inhibition and enhancement. Bordetella PTX was used first to prevent coupling of $G\alpha_{i/o}$ protein subunits to 5-HT receptors. Figure 4 shows an example of time courses of peak Ca^{2+} currents of a high responder (Fig. 4A) and enhancer (Fig. 4C) of the prepulse (●) and postpulse (○) currents evoked every 10 seconds with the triple-pulse voltage protocol shown (top right side, Fig. 4A). The corresponding numbered traces are shown to the right. Prior to 5-HT (10 μM) application, it can be seen that both prepulse and postpulse currents (traces 1 and 2) display slight inactivation. After 5-HT exposure, the rising phase of the prepulse (trace 3) exhibited kinetic slowing, a result of voltage-dependent relief of the block during the test pulse (Ikeda and Dunlap, 1999; Lu and Ikeda, 2016). Figure 4B shows a time course peak Ca^{2+} currents of a DiI-labeled DRG neuron pretreated overnight with PTX. It can be observed that the 5-HT-mediated inhibition was almost abolished (Fig. 4B, traces 3 and 4). The time course of an enhancer DiI-labeled DRG neuron before (traces 1 and 2) and during (traces 3 and 4) application of 5-HT is shown in Fig. 4C. It can be observed that 5-HT exposure led to an 11% enhancement of the currents in the presence of the agonist. Further, the overnight pretreatment with PTX of an enhancer neuron did not overtly affect the 5-HT-mediated $Ca_V2.2$ enhancement (Fig. 4D). That is, 5-HT application resulted in an 8% Ca^{2+} current enhancement. It should be noted that we could not predict a priori whether the total absence or diminished 5-HT-mediated $Ca_V2.2$ modulation after PTX treatment was due to selection of nonresponders or uncoupling of $G\alpha_{i/o}$ proteins to Ca^{2+} channels in either low or high responders. The results further indicate that enhancement of Ca^{2+} currents were unaffected by PTX treatment. Both the summary bars and pie charts in Fig. 4E summarize the frequency of the four responses to 5-HT observed in control and PTX-treated DRG neurons. The frequency of responses in the control

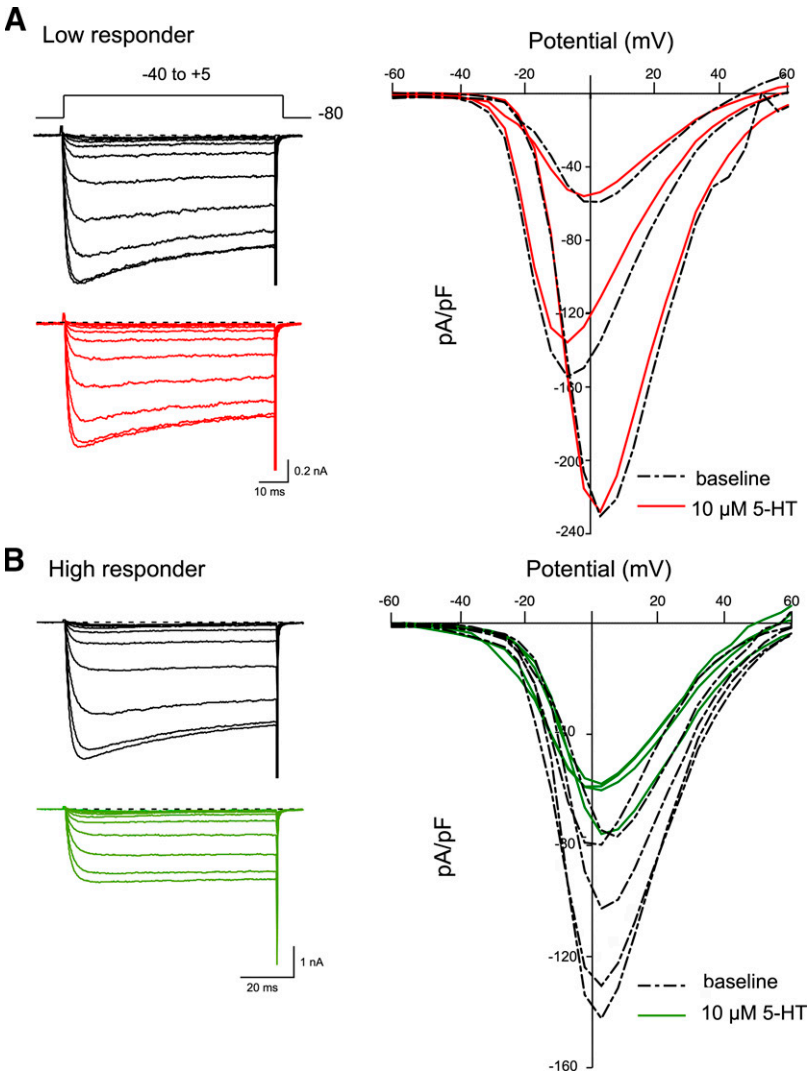

Fig. 2. The effect of 5-HT on the I-V relationships of acutely isolated DiI-labeled DRG neurons. Representative family of $Ca_V2.2$ currents evoked with the voltage protocol shown (A, top) in DRG neurons displaying low inhibition (A) and high inhibition (B). The currents were evoked every 5 seconds with a 70-millisecond pulse from −60 to +60 mV from a holding potential of −80 mV in the absence (black dash lines) and presence (red solid lines for low responders and green solid lines for high responders) of 5-HT (10 μM). The superimposed current traces shown were obtained with the test potentials ranging from −40 to +5 mV. I-V relationships (right side) for low responders (n = 3) and high responders (n = 5) groups depicted as spaghetti plots of the mean Ca^{2+} current density (pA/pF) for each test potential (mV).

group (Fig. 4E) are similar to those described in Fig. 1B. In the PTX-treated group of neurons, on the other hand, it can be seen that the frequency of low responders and high responders was decreased. The mean (±S.E.) 5-HT-mediated Ca^{2+} current inhibition in the nonresponders group was 2.5 ±1.0% (n = 13). In two neurons, the percent of Ca^{2+} current inhibition observed were 8% and 13%. These two latter neurons could represent either low responders resistant to PTX or high responders that are PTX-sensitive. All other factors being equal, these results suggest the voltage-dependent inhibition of $Ca_V2.2$ by 5-HT likely involves $G\alpha_{i/o}$ proteins, whereas a separate signaling pathway is responsible for Ca^{2+} current enhancement.

In another set of experiments, DiI-labeled DRG neurons were pretreated overnight with CTX to determine whether enhancement of $Ca_V2.2$ currents occurred via stimulation of $G\alpha_S$ protein subunits. This pretreatment with CTX locks the $G\alpha_S$ subunit in the guanosine 5'-triphosphate-bound state, which inhibits coupling to G protein-coupled receptors (Lu and Ikeda, 2016). Figure 5, A and B show peak Ca^{2+} currents elicited with a single-pulse voltage protocol (Fig. 5A, top) in a low responder (top) and an enhancer (bottom) in control and CTX-pretreated neurons, respectively. The superimposed current traces show peak Ca^{2+} currents before (black) and during (red or blue) 5-HT (10 μM) application. The summary pie charts in Fig. 5C show that the frequency of the four types of responses is comparable in the control and CTX groups. The results from this set of experiments indicate that $G\alpha_S$ proteins do not appear to couple 5-HT receptors with $Ca_V2.2$ in DRG neurons.

5-HT Receptor Subtype Expression in DiI-Labeled DRG Neurons. Given that PTX pretreatment abolished coupling of 5-HT receptors with $Ca_V2.2$, the next set of experiments was performed to identify the specific receptor subtype mediating the current modulation. Both 5-HT1 and 5-HT5 receptor subtypes employ $G\alpha_{i/o}$ protein subunits (Raymond et al., 2001). However, the 5-HT5 receptor subtype has been reported to be expressed during development stage of sensory neurons (Pierce et al., 1996; Nicholson et al., 2003). Therefore, these experiments focused on employing specific 5-HT1 receptor subtype pharmacological agents. We initially examined whether the repeated exposure to 5-HT (10 μM) produced robust and reproducible Ca^{2+} current inhibition. The time course in Fig. 6A shows the peak $Ca_V2.2$ currents evoked every 10 seconds as described for Fig. 1 above. The initial application of 5-HT resulted in an approximate Ca^{2+}

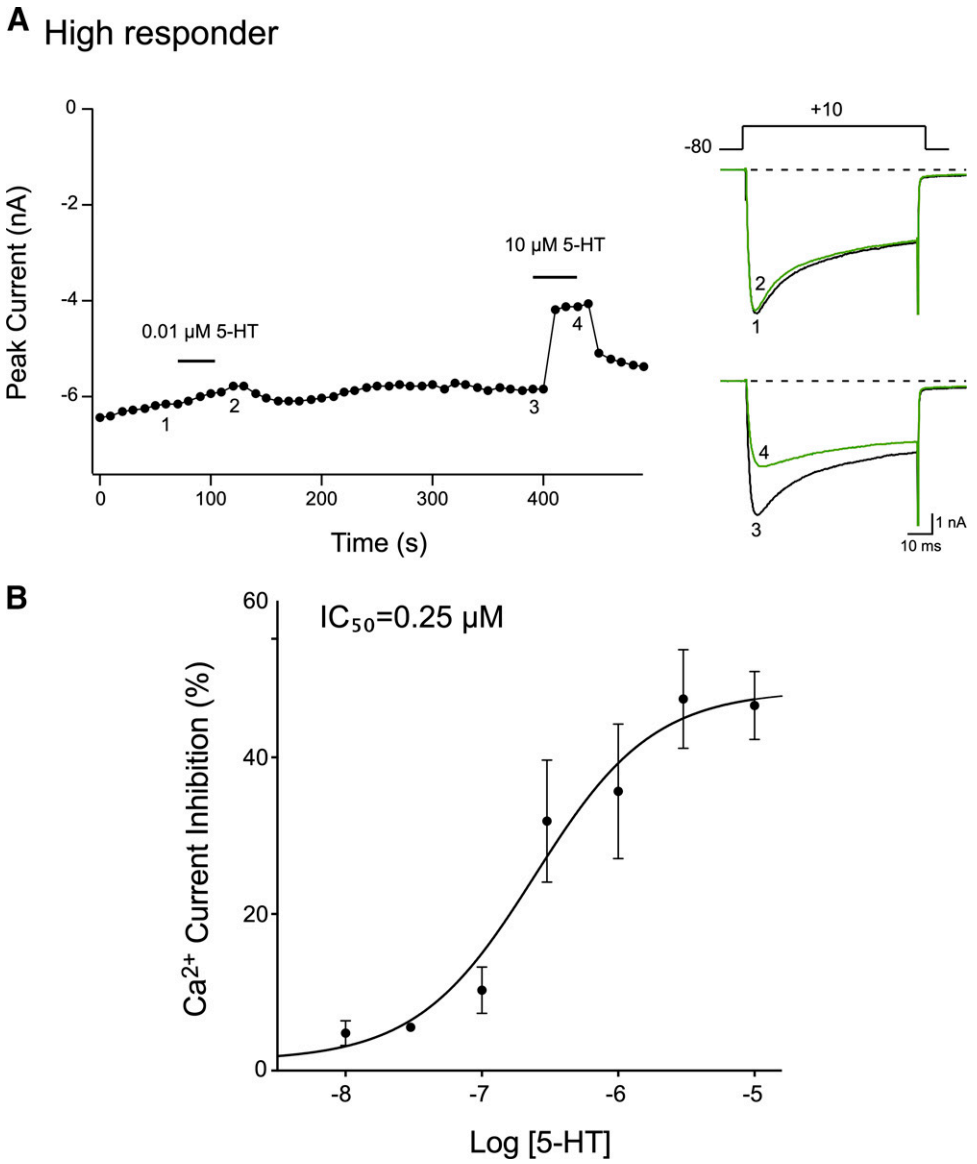

Fig. 3. 5-HT concentration-response relationships of high responder DiI-labeled DRG neurons. (A) Time course of peak $Ca_V2.2$ amplitude inhibition acquired from the sequential application of 0.01 and 10 μM 5-HT to a high responder DRG neuron. The superimposed current traces to the right were evoked every 10 seconds with the voltage protocol shown (A, top right). (B) 5-HT concentration-response relationships obtained for high responder DRG neurons. Each data point represents the mean (±S.E., n = 5–15, except 0.03 μM where n = 1) 5-HT-mediated current inhibition. The smooth curve was obtained by fitting the points to the Hill equation.

current block of 30% (traces 1 and 2), and re-exposure to 5-HT led to a 26% (traces 3 and 4) inhibition of the peak Ca^{2+} current (Fig. 6A). In four DRG neurons tested, the Ca^{2+} current inhibition was 23.8 ±8.5% and 23.5 ±8.3% after the first and second application of 5-HT, respectively. However, it is still possible that slight desensitization may occur as a result of the agonist concentration employed.

Figure 6Bi is a time course of peak $Ca_V2.2$ currents of a high responder neuron before and during exposure to either 5-HT (10 μM) or 5-HT and the specific 5-HT1A receptor blocker, NAD299 (30 μM). The plot indicates that an initial application of 5-HT blocked the Ca^{2+} currents by approximately 39%. After recovery, NAD299 was applied for approximately 3 minutes, followed by coexposure to NAD299 and 5-HT. The 5-HT-mediated Ca^{2+} current inhibition was reduced in the presence of the 5-HT1A receptor blocker to 4%. The summary plot shown in Fig. 6Bii shows that NAD299 significantly ($P < 0.05$) blocked the 5-HT-mediated $Ca_V2.2$ block. Additional experiments were performed with low responder neurons. The findings are summarized in Fig. 6Biii. NAD299 exhibited a similar significant ($P < 0.05$) blocking effect of the 5-HT-mediated Ca^{2+} current inhibition as that observed with high responder neurons.

In the next series of experiments, the use of the selective 5-HT1B and 5-HT1D receptor blockers, NAS181 and LY310762 (30 μM), respectively, on high responder and low responder neurons was performed. The summarized findings (Fig. 6, Ci–Ciii) for NAS181 indicate that 5-HT does not appear to modulate $Ca_V2.2$ via 5-HT1B receptors since the modulation of the currents remained unaltered. On the other hand, the use of the 5-HT1D blocker led to a significant ($P < 0.05$) reduction in the 5-HT-mediated Ca^{2+} current inhibition in high responder neurons (Fig. 6, Di and Dii), suggesting that the 5-HT1D receptor subtype couples with $Ca_V2.2$. In

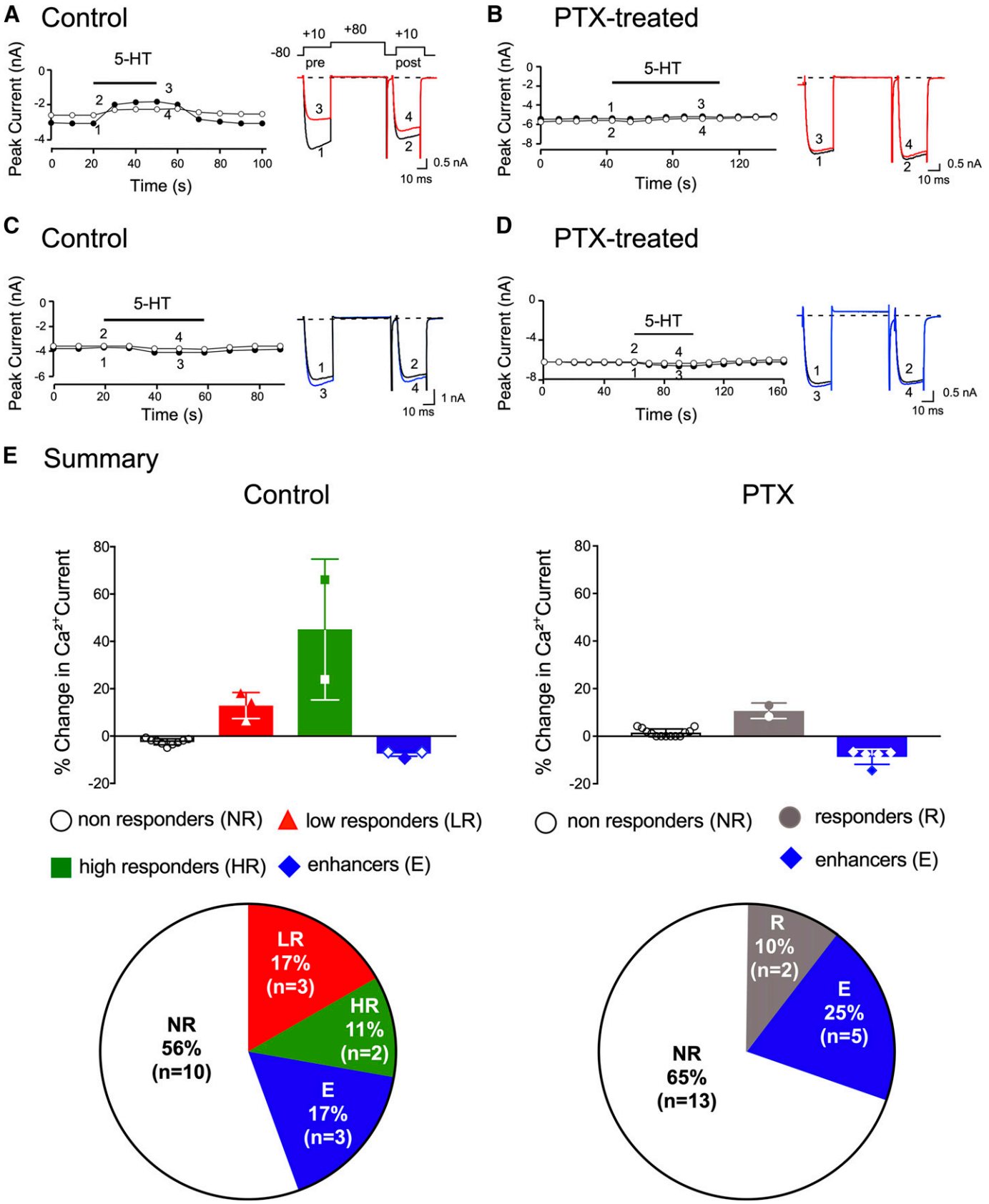

Fig. 4. 5-HT-mediated $Ca_V2.2$. inhibition is PTX-sensitive. Time courses of Ca^{2+} current amplitude for prepulse (●) and postpulse (○) acquired before and during application of 5-HT (10 μM) in control (A, C) and neurons pretreated overnight with PTX (500 ng/ml) for high responder (B) or enhancer (D). The superimposed current traces were obtained with the triple-pulse voltage protocol shown (top right side) before (traces 1 and 2) and in the presence of 5-HT (traces 3 and 4). The Ca^{2+} currents were evoked every 10 seconds. (E) Summary bar graphs showing mean (±S.D.) and pie charts showing the fractional representation of the observed effects mediated by 5-HT on $Ca_V2.2$ currents in control or PTX-treated DiI-labeled DRG neurons. The numbers in parentheses indicate the number of neurons tested.

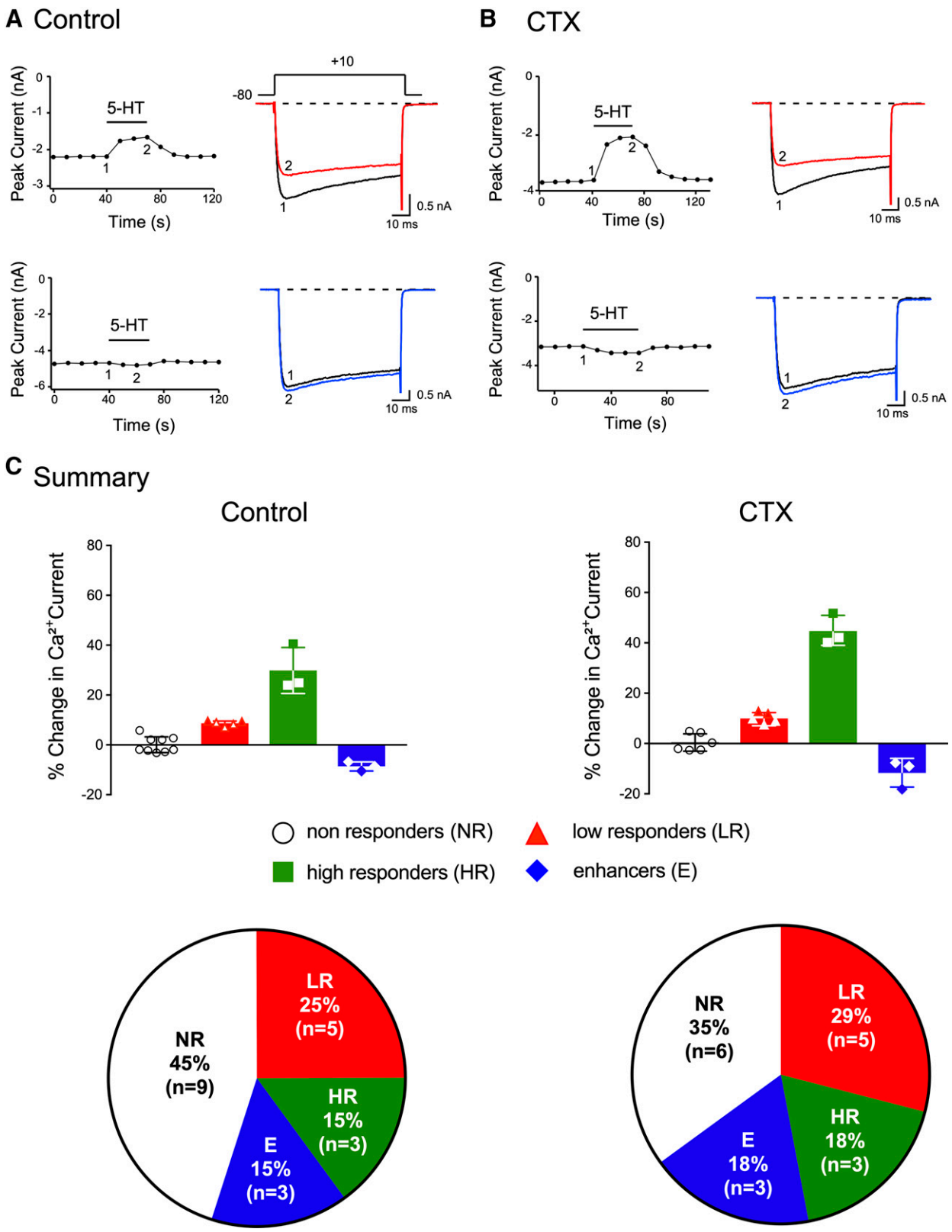

Fig. 5. 5-HT-mediated $Ca_V2.2$ inhibition and enhancement is CTX-resistant. Time courses of Ca^{2+} current amplitude acquired from the application of 5-HT (10 μM) in control neurons (A) and in DRG neurons pretreated overnight with CTX (500 ng/ml, B) for both low responder (top) or enhancer (bottom). The superimposed current traces were obtained with the single-pulse voltage protocol shown (top right side) before (trace 1) and in the presence of 5-HT (trace 2). The Ca^{2+} currents were evoked every 10 seconds. (C) Summary bar graphs showing mean (±S.D.) and pie charts showing the fractional representation of the observed 5-HT-mediated effects on $Ca_V2.2$ currents in control and CTX-treated DiI-labeled DRG neurons. The numbers in parentheses indicate the number of neurons tested.

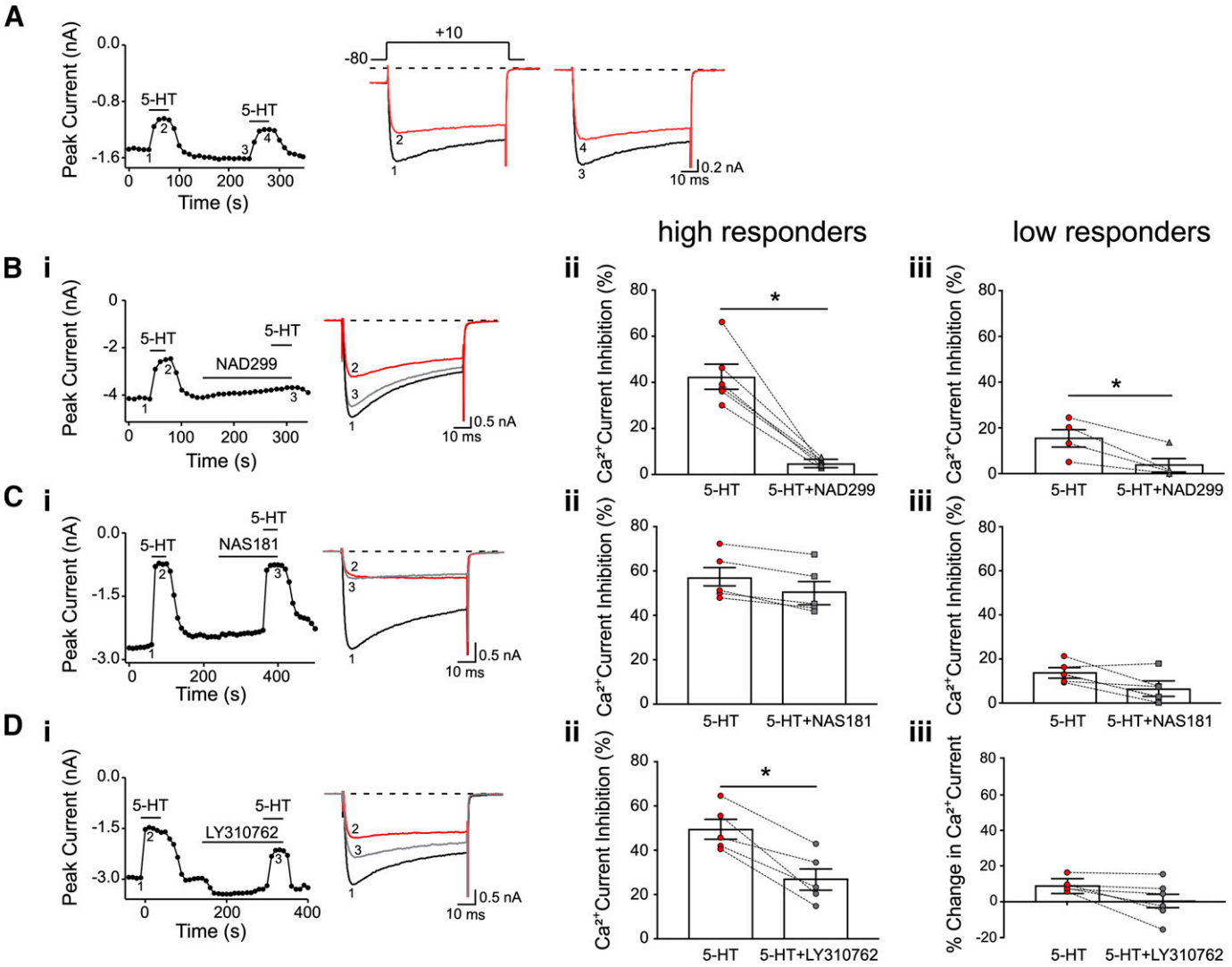

Fig. 6. Pharmacological profile of 5-HT1 receptors in acutely dissociated high responder and low responder DRG neurons. (A) Time course of peak $Ca_V2.2$ current inhibition acquired from the sequential application of 5-HT (10 μM) in a DRG neuron. On the right are superimposed Ca^{2+} current traces evoked with the voltage protocol (top) before (control trace 1 and 3), in the presence of 5-HT (trace 2 and 4). Currents were evoked every 10 seconds by a single 70-millisecond pulse to +10 mV from a holding potential of −80 mV. (Bi) Time course of peak $Ca_V2.2$ current inhibition acquired from the sequential application of 5-HT (10 μM) and 5-HT in presence of NAD299 (30 μM) in a high responder DRG neuron. On the right are superimposed Ca^{2+} current traces evoked with the voltage protocol (top) before (control trace 1), in the presence of 5-HT (trace 2), and 5-HT in presence of NAD299 (trace 3). Currents were evoked every 10 seconds by a single 70-millisecond pulse to +10 mV from a holding potential of −80 mV. (Bii and Biii) Summary dot plots of mean (±S.E.) Ca^{2+} current inhibition produced by application of 5-HT (red) and 5-HT with NAD299 (gray) in high responder (n = 6) and low responder (n = 4) DRG neurons. (Bi) Time course of peak $Ca_V2.2$ current inhibition acquired from the sequential application of 5-HT (10 μM) and 5-HT in presence of NAS181 (30 μM) of a high responder DRG neuron. The superimposed Ca^{2+} current traces to the right were evoked as described in Ai in the presence of 5-HT (trace 2) and 5-HT and NAS181 (trace 3). (Cii and Ciii) Summary dot plots of mean (±S.E.) Ca^{2+} current inhibition produced by application of 5-HT (red) and 5-HT with NAS181 (gray) in high responder (n = 5) and low responder (n = 6) DRG neurons. (Di) Time course of peak $Ca_V2.2$ current inhibition acquired from the sequential application of 5-HT (10 μM) and 5-HT in presence of LY310762 (30 μM) of a high responder DRG neuron. The superimposed Ca^{2+} current traces to the right were evoked as described in Ai in the presence of 5-HT (trace 2) and 5-HT and LY310762 (trace 3). (Dii and Diii) Summary dot plots of mean (±S.E.) Ca^{2+} current inhibition produced by application of 5-HT (red) and 5-HT with LY310762 (gray) in high responder (n = 5) and low responder (n = 6) DRG neurons. * indicates $P < 0.05$ employing a paired t test.

addition, in the low responder group coexposure of LY310762 with 5-HT did not overtly affect the mean Ca^{2+} current inhibition. However, we observed that Ca^{2+} currents were slightly enhanced in three of the six neurons tested (Fig. 6Diii). Thus, 5-HT1D receptor subtypes likely do not modulate $Ca_V2.2$ in the low responder group.

Presynaptic Spinal 5-HT1A Receptor Stimulation Inhibits Pressor Response to Lactic Acid. Our electrophysiological findings suggested that 5-HT1A stimulation caused the majority of $Ca_V2.2$ inhibition of DiI-labeled neurons innervating triceps surae muscle with a partial contribution of 5-HT1D receptors. Thus, in vivo experiments were performed to determine the effect of 5-HT receptor stimulation with intrathecal administration of either 5-HT or the selective 5-HT1A receptor agonist on the lactic acid-mediated evoked increase in blood pressure. In preliminary experiments, we tested the effect of intrathecal vehicle administration for 5-HT (saline) and 8OH-DPAT (6% DMSO) on blood pressure alone. In five rats, saline injection resulted in a mean arterial pressure (MAP) change (±S.E.) from

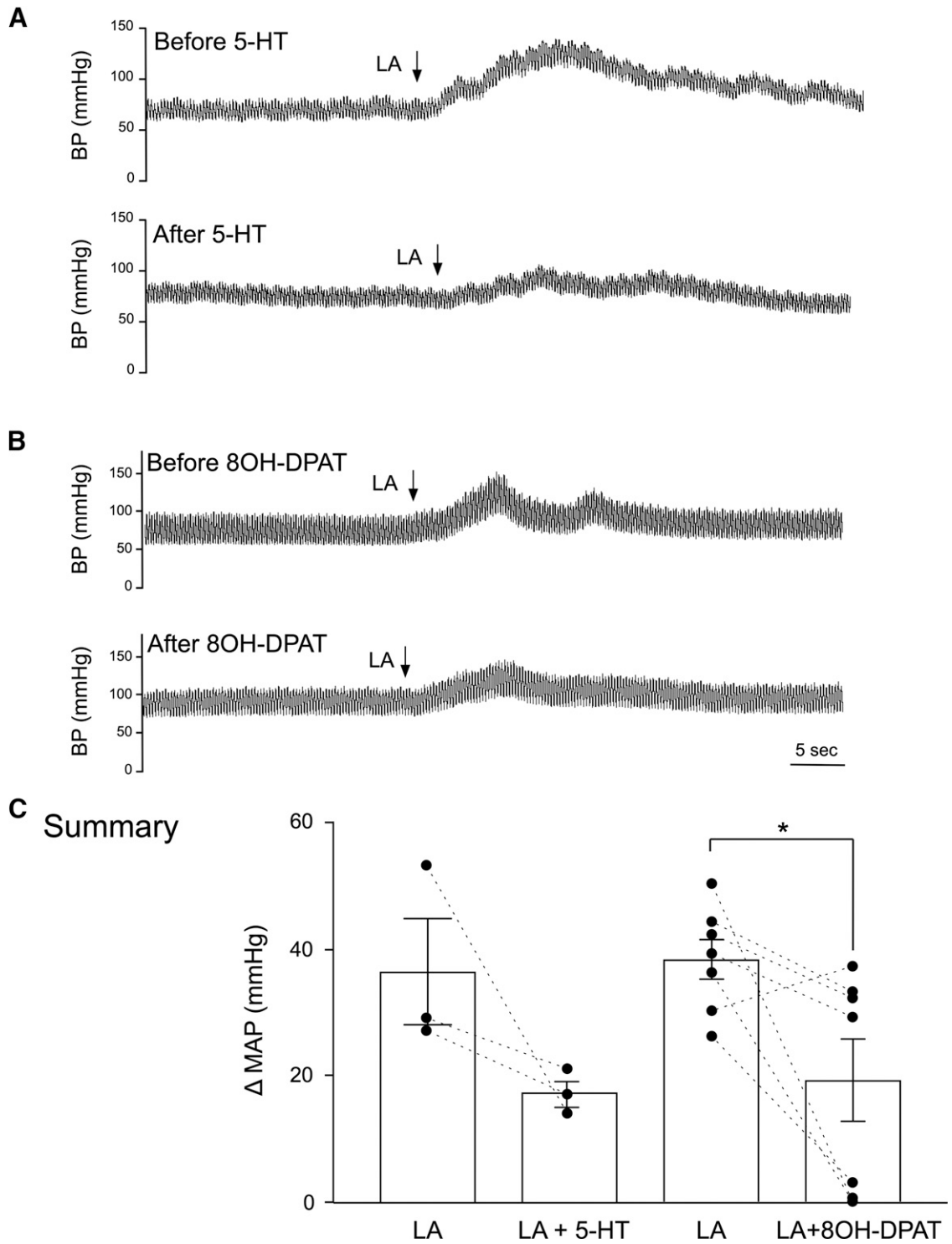

Fig. 7. 8OH-DPAT pretreatment ameliorates the lactic acid-induced increase in mean arterial pressure. (A) and (B) Blood pressure (BP) responses to intra-arterial infusion of lactic acid (LA, 12 mM) in a rat before and after intrathecal administration of 5-HT (25 μg, A) and 8OH-DPAT (50 μg, B). (C) Summary plot showing the mean change (±S.E.) in MAP after intra-arterial infusion of LA alone and after intrathecal administration of either 5-HT (25 μg, $n = 3$) or 8OH-DPAT (50 μg, $n = 7$). * indicates $P < 0.05$ employing a paired t test.

43 ±16 mmHg to 38 ± 9 mmHg ($P = 0.65$, t test). In addition, in three rats, 6% DMSO administration led to a mean MAP (±S.E.) change from 38 ±4 mmHg to 44 ±6 mmHg ($P = 0.41$, t test). Figure 7A (top) shows an increase in blood pressure from 73 to 126 mmHg (a change of 53 mmHg) after an intra-arterial injection of lactic acid (12 mM) prior to 5-HT (25 μg) administration. This concentration of lactic acid has been previously shown to be comparable to rat plasma levels obtained during strenuous exercise (Madureira and Hasson-Voloch, 1988). After a recovery period, an intrathecal injection of the 5-HT was performed (Fig. 7a, bottom). Thereafter, lactic acid was administered intra-arterially again, and blood pressure was increased from 80 to 94 mmHg (a change of 14 mmHg). Figure 7B shows the blood pressure response to

intra-arterial lactic acid administration before (top) and after (bottom) intrathecal application of the selective 5-HT1A receptor agonist, 8OH-DPAT. It can be observed that the lactic acid-mediated increase in blood pressure was reduced in the presence of 8OH-DPAT when compared with the control response (81 to 125 mmHg in control versus 80 to 113 mmHg). The summary plot in Fig. 7C shows the change in MAP. The results indicate that, unlike the global stimulation of 5-HT receptors by 5-HT, stimulation of 5-HT1A receptors after intrathecal administration of 8OH-DPAT significantly ($P < 0.05$) reduced the lactic acid-mediated increase in blood pressure, presumably via presynaptic block of $Ca_V2.2$ in group III and IV afferents (Kim and Kaufman, 2019).

Discussion

It is well established that the exercise pressor reflex plays a key role in both enhanced cardiovascular and pulmonary function during exercise. This sensory reflex results from chemo- and mechanosensory stimulation of group III and IV afferents innervating the contracting skeletal muscle (Kaufman et al., 1983). Some of the metabolites released during muscle contraction include lactic acid, 5-HT, ATP, bradykinin, arachidonic acid, and its cyclooxygenase metabolites (Kaufman et al., 1983; Rotto and Kaufman, 1988; Hill and Kaufman, 1991; Hanna and Kaufman, 2004). However, some of these metabolites, including 5-HT, can also affect neuronal excitability presynaptically at the spinal cord (Hill and Kaufman, 1991; Nobrega et al., 1995). Previously, we reported that intrathecal injection of 5-HT onto the lumbosacral spinal cord attenuated the reflex pressor response to static muscle contraction (Hill and Kaufman 1991). In the present study, we focused on delineating the 5-HT signaling pathways and pharmacology of sensory afferents involved in regulating the pressor responses to muscle exercise. Therefore, our aims were first to determine the effect of 5-HT on $Ca_V2.2$ currents in rat DRG neurons innervating the triceps surae muscle; second, to identify the signaling components and specific 5-HT receptors that are coupled to $Ca_V2.2$; and third, to examine whether intrathecal block of 5-HT receptors would alter the pressor response after intra-arterial lactic acid administration.

An unexpected finding in this study was the 5-HT-mediated enhancement of Ca_V currents in approximately 15% of DRG neurons tested. The modulation of $Ca_V2.2$ after G-protein coupled receptor stimulation is typically associated with either voltage-dependent or voltage-independent Ca_V block (Ikeda and Dunlap, 1999; Elmslie, 2003). The enhancement of the Ca^{2+} currents was not affected by either PTX or CTX pretreatment, suggesting that $G\alpha_{i/o}$ and $G\alpha_S$ protein subfamilies do not contribute to this signaling pathway. The lack of specific blockers for other $G\alpha$ protein subfamilies, such as $G\alpha_{q/11}$ and $G\alpha_{14}$, precluded us from testing whether they are involved in this pathway. Based on a previous report (Su et al., 2012), we surmise that the current enhancement was likely a result of channel phosphorylation. In that study, $Ca_V2.2$ were heterologously expressed in temperature-sensitive T-antigen cells, and it was shown that the channels served as substrates for cyclin-dependent kinase 5 (CDK5), such that channel phosphorylation led to an increase in both $Ca_V2.2$ current density and open probability (Su et al., 2012). CDK5 is an important regulator of neuronal functions, including synaptic activity, neurite outgrowth, pain signaling, survival, and death (Utreras et al., 2009; Hisanaga and Endo, 2010; Pareek et al., 2013; Takahashi et al., 2019). Another study showed that CDK5 overexpression in N1E-115 cells caused a substantial increase in $Ca_V3.1$ channel currents (Calderón-Rivera et al., 2015). In both reports, however, the physiologic correlate was not identified. Given that CDK5 has been reported to mediate the phosphorylation-dependent degradation of 5-HT1A receptors (Takahashi et al., 2019), it is probable that this protein kinase modulates the 5-HT1A/$Ca_V2.2$ receptor signaling pathway. For instance, under inflammatory conditions, such as PAD, CDK5 controls afferent excitability via phosphorylation of both $Ca_V2.2$ and 5-HT1A.

A second unexpected finding was that $Ca_V2.2$ inhibition after 5-HT receptor stimulation occurred in either a high or low manner. These observations were not a result of receptor desensitization, but rather they represent two distinct DRG subpopulations, as identified by the random effects finite mixture regression model showing clusters of different upward patterns with increased dose levels. The observation frequency for low responder population was higher than that observed with the high responder group (23% versus 13%). It should be noted that we were unable to generate a 5-HT concentration-response relationship for the low responder group as the dynamic range for Ca^{2+} channel block observed was small with agonist concentrations employed (0.01 to 10 μM). Also, at high concentrations, 5-HT may have exerted nonspecific effects. Nevertheless, PTX pretreatment decreased substantially the 5-HT-mediated block of Ca^{2+} currents for both groups of neurons, whereas CTX was without effect. This suggests that both high and low responders employ $G\alpha_{i/o}$-coupled signaling elements. However, a limited number of neurons were tested with both toxins.

We also found that modulation of $Ca_V2.2$ currents after 5-HT exposure was not observed in approximately 50% of DiI-labeled neurons tested. This does not necessarily indicate that other 5-HT receptor subtypes are not expressed. It is possible that other 5-HT receptor subtypes do not couple to $Ca_V2.2$. For instance, 5-HT has also been shown to increase DRG excitability via 5-HT2C-mediated opening of Ca^{2+}-activated chloride channels (Salzer et al., 2016). Alternatively, the DiI-labeled neurons may express ionotropic 5-HT3 receptors. We did not, however, examine the effect of 5-HT on these ligand-activated currents.

Previously, it had been reported that DRG neurons express 5-HT1–5HT5 and 5-HT7 receptor subtypes (Daval et al., 1987; Cardenas et al., 1997a; Cardenas et al., 1997b; Chen et al., 1998; Classey et al., 2010). Our pharmacological findings show that DRG neurons innervating triceps surae muscle employ primarily 5-HT1A and 5-HT1D to effect $Ca_V2.2$. Nevertheless, we cannot rule out that the $G\alpha_{i/o}$-coupled 5HT-5 receptor subtype is not expressed in DRG. It is possible that this receptor subtype does not modulate $Ca_V2.2$ currents, or its expression levels are low under our experimental conditions (i.e., adult neurons). This receptor subtype is believed to play a role in development (Nicholson et al., 2003). Additional experiments with specific 5HT-5 receptor agonists and antagonists are necessary to determine whether DRG neurons innervating hindlimb muscle express this receptor subtype.

Our results also show that application of the selective 5-HT1A receptor blocker, NAD299, exhibited a greater block of the 5-HT-mediated $Ca_V2.2$ inhibition than the selective 5-HT1D receptor blocker, LY310762. The reported inhibition constant values are 0.59 nM and and 249 nM, respectively, for NAD299 and LY310762 (Johansson et al., 1997; Pullar et al., 2004). However, in the present study, we employed 30 μM of all antagonists to block the 5-HT mediated Ca^{2+} current inhibition. Therefore, we cannot rule out the possibility that these blockers may have exerted nonspecific effects, such as binding to other receptors. Similarly, exposure of the DiI-labeled DRG neurons to the 5-HT1B receptor antagonist, NAS181, was without effect. However, the reported inhibition constant for this blocker is 47 nM (Berg et al., 1998). It is also possible that NAS181 could have caused nonspecific actions and is a limitation of the study.

Finally, our in vivo findings suggest that 5-HT1A receptors are present presynaptically on afferents projecting to the spinal cord, as intrathecal application of either 5-HT or 8OH-DPAT (selective 5-HT1A receptor agonist) inhibited the lactic acid-induced pressor reflex. Previously, we showed that intrathecal injections of 5-HT attenuated the reflex pressor response to static contraction of the triceps surae muscle in cats (Hill and Kaufman, 1991). This seems to suggest that the pressor responses in both species are modulated by 5-HT1A receptors.

In summary, our results show that the neurotransmitter 5-HT can differentially modulate $Ca_V2.2$ currents in rat DRG neurons innervating triceps surae muscle. In DiI-labeled neurons, 5-HT exposure either enhanced or blocked $Ca_V2.2$, the latter via $G\alpha_{i/o}$ subunits coupled to 5-HT1A and 5-HT1D receptor subtypes. The $Ca_V2.2$ current block was observed in two distinct DRG subtypes—low and high responders. That 5-HT can mediate opposite actions in neurons innervating triceps surae muscle is a conundrum. DRG neurons are structurally classified as unipolar from which a single process leaves the soma and then divides to supply dendritic terminals to tissues (i.e., muscle) and axons that terminate in the spinal cord. It is tempting to speculate that under heavy exercise or ischemia or inflammation, 5-HT release (among other mediators) within muscle stimulates 5-HT1A receptors that enhance $Ca_V2.2$ currents and, thereby, excitability, of group III and IV afferents. As the signal travels to the soma and ends at the presynaptic terminal, 5-HT release by the dorsal raphe nuclei stimulates 5-HT1A receptors that are coupled to $G\alpha_{i/o}$ subunits and block $Ca_V2.2$ currents. The result is a decrease of neurotransmitter release and synaptic transmission with a concomitant reduction of the pressor reflex.

Authorship Contributions

Participated in research design: Anselmi, Kaufman, Ruiz-Velasco.

Conducted experiments: Anselmi, Kim.

Performed data analysis: Anselmi, Zhou.

Wrote or contributed to the writing of the manuscript: Anselmi, Kaufman, Kim, Ruiz-Velasco, Zhou.

Acknowledgments

The authors thank Paul B. Herold for excellent technical support.

References

Bardin L (2011) The complex role of serotonin and 5-HT receptors in chronic pain. *Behav Pharmacol* **22**:390–404.

Berg S, Larsson L-G, Rényi L, Ross SB, Thorberg S-O, and Thorell-Svantesson G (1998) (R)-(+)-2-[[[3-(Morpholinomethyl)-2H-chromen-8-yl]oxy]methyl] morpholine methanesulfonate: a new selective rat 5-hydroxytryptamine$_{1B}$ receptor antagonist. *J Med Chem* **41**:1934–1942.

Calderón-Rivera A, Sandoval A, González-Ramírez R, González-Billault C, and Felix R (2015) Regulation of neuronal cav3.1 channels by cyclin-dependent kinase 5 (Cdk5). *PLoS One* **10**:e0119134.

Cardenas CG, Del Mar LP, Cooper BY, and Scroggs RS (1997a) 5HT4 receptors couple positively to tetrodotoxin-insensitive sodium channels in a subpopulation of capsaicin-sensitive rat sensory neurons. *J Neurosci* **17**:7181–7189.

Cardenas CG, Del Mar LP, and Scroggs RS (1997b) Two parallel signaling pathways couple 5HT1A receptors to N- and L-type calcium channels in C-like rat dorsal root ganglion cells. *J Neurophysiol* **77**:3284–3296.

Chen JJ, Vasko MR, Wu X, Staeva TP, Baez M, Zgombick JM, and Nelson DL (1998) Multiple subtypes of serotonin receptors are expressed in rat sensory neurons in culture. *J Pharmacol Exp Ther* **287**:1119–1127.

Classey JD, Bartsch T, and Goadsby PJ (2010) Distribution of 5-HT(1B), 5-HT(1D) and 5-HT(1F) receptor expression in rat trigeminal and dorsal root ganglia neurons: relevance to the selective anti-migraine effect of triptans. *Brain Res* **1361**:76–85.

Cortes-Altamirano JL, Olmos-Hernandez A, Jaime HB, Carrillo-Mora P, Bandala C, Reyes-Long S, and Alfaro-Rodríguez A (2018) Review: 5-HT1, 5-HT2, 5-HT3 and 5-HT7 receptors and their role in the modulation of pain response in the central nervous system. *Curr Neuropharmacol* **16**:210–221.

Daval G, Vergé D, Basbaum AI, Bourgoin S, and Hamon M (1987) Autoradiographic evidence of serotonin1 binding sites on primary afferent fibres in the dorsal horn of the rat spinal cord. *Neurosci Lett* **83**:71–76.

De Ponti F (2004) Pharmacology of serotonin: what a clinician should know. *Gut* **53**:1520–1535.

Derkach V, Surprenant A, and North RA (1989) 5-HT3 receptors are membrane ion channels. *Nature* **339**:706–709.

Elmslie KS (2003) Neurotransmitter modulation of neuronal calcium channels. *J Bioenerg Biomembr* **35**:477–489.

Farrag M, Drobish JK, Puhl HL, Kim JS, Herold PB, Kaufman MP, and Ruiz-Velasco V (2017) Endomorphins potentiate acid-sensing ion channel currents and enhance the lactic acid-mediated increase in arterial blood pressure: effects amplified in hindlimb ischaemia. *J Physiol* **595**:7167–7183.

Hanna RL and Kaufman MP (2004) Activation of thin-fiber muscle afferents by a P2X agonist in cats. *J Appl Physiol (1985)* **96**:1166–1169.

Hassan B, Kim JS, Farrag M, Kaufman MP, and Ruiz-Velasco V (2014) Alteration of the mu opioid receptor: Ca^{2+} channel signaling pathway in a subset of rat sensory neurons following chronic femoral artery occlusion. *J Neurophysiol* **112**:3104–3115.

Hill JM and Kaufman MP (1991) Intrathecal serotonin attenuates the pressor response to static contraction. *Brain Res* **550**:157–160.

Hisanaga S and Endo R (2010) Regulation and role of cyclin-dependent kinase activity in neuronal survival and death. *J Neurochem* **115**:1309–1321.

Hornung J-P (2003) The human raphe nuclei and the serotonergic system. *J Chem Neuroanat* **26**:331–343.

Hoyer D, Hannon JP, and Martin GR (2002) Molecular, pharmacological and functional diversity of 5-HT receptors. *Pharmacol Biochem Behav* **71**:533–554.

Ikeda SR (1991) Double-pulse calcium channel current facilitation in adult rat sympathetic neurones. *J Physiol* **439**:181–214.

Ikeda SR and Dunlap K (1999) Voltage-dependent modulation of N-type calcium channels: role of G protein subunits. *Adv Second Messenger Phosphoprotein Res* **33**:131–151.

Johansson L, Sohn D, Thorberg S-O, Jackson DM, Kelder D, Larsson L-G, Rényi L, Ross SB, Wallsten C, Eriksson H, et al. (1997) The pharmacological characterization of a novel selective 5-hydroxytryptamine$_{1A}$ receptor antagonist, NAD-299. *J Pharmacol Exp Ther* **283**:216–225.

Kaufman MP, Longhurst JC, Rybicki KJ, Wallach JH, and Mitchell JH (1983) Effects of static muscular contraction on impulse activity of groups III and IV afferents in cats. *J Appl Physiol* **55**:105–112.

Kim JS and Kaufman MP (2019) Stimulation of spinal δ-opioid receptors attenuates the exercise pressor reflex in decerebrate rats. *Am J Physiol Regul Integr Comp Physiol* **316**:R727–R734.

Lu VB and Ikeda SR (2016) Strategies for investigating G-protein modulation of voltage-gated Ca^{2+} channels. *Cold Spring Harb Protoc* **2016**:426–434.

Madureira G and Hasson-Voloch A (1988) Lactate utilization and influx in resting and working rat red muscle. *Comp Biochem Physiol A Comp Physiol* **89**:693–698.

McLachlan GJ and Peel D (2000) *Finite Mixture Models*, John Wiley & Sons, New York.

Millan MJ, Marin P, Bockaert J, and Mannoury la Cour C (2008) Signaling at G-protein-coupled serotonin receptors: recent advances and future research directions. *Trends Pharmacol Sci* **29**:454–464.

Nicholson R, Small J, Dixon AK, Spanswick D, and Lee K (2003) Serotonin receptor mRNA expression in rat dorsal root ganglion neurons. *Neurosci Lett* **337**:119–122.

Nóbrega AC, Meintjes AF, Ally A, and Wilson LB (1995) Modulation of reflex pressor response to contraction and effect on substance P release by spinal 5-HT1A receptors. *Am J Physiol* **268**:H1577–H1585.

Pareek TK, Zipp L, and Letterio JJ (2013) Cdk5: an emerging kinase in pain signaling. *Brain Disord Ther* **2013** (Suppl 1):1–17.

Pierce PA, Xie GX, Levine JD, and Peroutka SJ (1996) 5-Hydroxytryptamine receptor subtype messenger RNAs in rat peripheral sensory and sympathetic ganglia: a polymerase chain reaction study. *Neuroscience* **70**:553–559.

Pullar IA, Boot JR, Broadmore RJ, Eyre TA, Cooper J, Sanger GJ, Wedley S, and Mitchell SN (2004) The role of the 5-HT$_{1D}$ receptor as a presynaptic autoreceptor in the guinea pig. *Eur J Pharmacol* **493**:85–93.

Ramachandra R, Hassan B, McGrew SG, Dompor J, Farrag M, Ruiz-Velasco V, and Elmslie KS (2013) Identification of CaV channel types expressed in muscle afferent neurons. *J Neurophysiol* **110**:1535–1543.
Raymond JR, Mukhin YV, Gelasco A, Turner J, Collinsworth G, Gettys TW, Grewal JS, and Garnovskaya MN (2001) Multiplicity of mechanisms of serotonin receptor signal transduction. *Pharmacol Ther* **92**:179–212.
Rotto DM and Kaufman MP (1988) Effect of metabolic products of muscular contraction on discharge of group III and IV afferents. *J Appl Physiol (1985)* **64**:2306–2313.
Salzer I, Gantumur E, Yousuf A, and Boehm S (2016) Control of sensory neuron excitability by serotonin involves 5HT2C receptors and Ca(2+)-activated chloride channels. *Neuropharmacology* **110** (Pt A):277–286.
Senol S and Es MU (2015) Is serotonin a valuable parameter in peripheral arterial disease? *Asian Cardiovasc Thorac Ann* **23**:289–291.
Shajib MS and Khan WI (2015) The role of serotonin and its receptors in activation of immune responses and inflammation. *Acta Physiol (Oxf)* **213**:561–574.
Sommer C (2004) Serotonin in pain and analgesia: actions in the periphery. *Mol Neurobiol* **30**:117–125.
Stojanović M, Prostran M, Janković R, and Radenković M (2017) Clarification of serotonin-induced effects in peripheral artery disease observed through the femoral artery response in models of diabetes and vascular occlusion: the role of calcium ions. *Clin Exp Pharmacol Physiol* **44**:749–759.
Su SC, Seo J, Pan JQ, Samuels BA, Rudenko A, Ericsson M, Neve RL, Yue DT, and Tsai L-H (2012) Regulation of N-type voltage-gated calcium channels and presynaptic function by cyclin-dependent kinase 5. *Neuron* **75**:675–687.
Švob Štrac D, Pivac N, and Mück-Šeler D (2016) The serotonergic system and cognitive function. *Transl Neurosci* **7**:35–49.
Takahashi M, Kobayashi Y, Ando K, Saito Y, and Hisanaga S-I (2019) Cyclin-dependent kinase 5 promotes proteasomal degradation of the 5-HT_{1A} receptor via phosphorylation. *Biochem Biophys Res Commun* **510**:370–375.
Utreras E, Futatsugi A, Pareek TK, and Kulkarni AB (2009) Molecular roles of Cdk5 in pain signaling. *Drug Discov Today Ther Strateg* **6**:105–111.
Watts SW, Morrison SF, Davis RP, and Barman SM (2012) Serotonin and blood pressure regulation. *Pharmacol Rev* **64**:359–388.
Westenbroek RE, Hoskins L, and Catterall WA (1998) Localization of Ca^{2+} channel subtypes on rat spinal motor neurons, interneurons, and nerve terminals. *J Neurosci* **18**:6319–6330.

Address correspondence to: Victor Ruiz-Velasco, Department of Anesthesiology and Perioperative Medicine, Penn State College of Medicine, 500 University Drive, H187, Hershey, PA 17033. E-mail: vruizvelasco@psu.edu